Microwave Interactions in Semiconductor Multiple-Quantum-Well Heterostructures Utilizing a Coplanar-Strip Geometry Device

Steven W. Kirchoefer, *Member, IEEE*

Abstract—**A novel device design utilizing a multiple-quantum-well heterostructure conduction channel with an oxide-isolated overlying coplanar-strip transmission line has been constructed. These devices exhibit negative differential conductance in their dc characteristics for current transport in the plane of the quantum-well layers, originating from the change in mobility of the heated electrons within the quantum-well structure. This device design has permitted the observation of nonlinear conduction properties using these multiple-quantum-well heterostructures at microwave frequencies.**

I. Introduction

NONLINEAR conduction effects in quantum-well heterostructure devices have been widely investigated for use in microwave applications. The microwave performance of prototype multiple-quantum-well heterojunction devices is typically limited to a few gigahertz by the parasitic effects that are always present in discrete device designs [1], [2]. The result is in an inability to characterize the frequency limitations of the underlying conduction processes in the pertinent structures. This paper reports on the use of a coplanar-strip fabrication technology to construct a novel coplanar stripline device and observe microwave properties at higher frequencies than can be accommodated with conventional nondistributed device designs.

A. DC Conduction in Multi-Level Quantum-Well Heterostructures

The basic concept behind the negative-conductivity properties of multiple-level quantum-well heterostructures is analogous to the concept underlying the Gunn effect. With the Gunn effect, electrons at low applied electric fields reside in the high-mobility low-energy Γ -minimum of the conduction band. When a sufficiently high electric field is applied, electrons become heated, and can make transitions from the Γ-minimum to the X-minima. Electrons in the X-minima have relatively low mobility and high energy compared to those in the Γ minimum. It is the co-existence of these low-energy, high-mobility states with high-energy, low-mobility states into which heated electrons can scatter that form the conceptual basis for the intervalley scattering model of the Gunn effect. Intervalley scattering is a k-space phenomena. Real-space analogs to intervalley scattering have also been demonstrated [3]–[5]. These concepts involve the use of heterostructure-growth technologies to realize materials that possess low-energy, high-mobility and high-energy, low-mobility states originating from real-space properties in these structures, rather than from k-space properties. Because the transitions between states occur in real space and not in k-space, one expects not to observe the domain-formation consequences of intervalley scattering. This lack of domain formation and the resulting uniform electric field distribution with applied bias makes these materials attractive for incorporation into distributed devices which stand to benefit from the spatial independence of the negative conductivity. A simple coplanar-strip transmission line represents such a device application, since the bias-dependent conductivity of the heterostructure appears to the transmission line as a substrate of variable-conductivity. By measuring the microwave properties of this transmission line while applying a dc electric field to the heterojunction, the microwave response of the quantum-well conduction as a function of the dc bias can be observed.

The manner in which one incorporates the necessary energy-state characteristics into a heterostructure design is straightforward. Many heterojunction materials have variable mobilities and bandgaps within lattice-matched composition ranges, and so offer the possibility of realizing a real-space device through composition variations in bulk heterojunction layers [3], [4]. Another method to realize these structures involves the use of quantum wells [5], [6]. Quantum wells are fabricated by sandwiching a low-energy-gap layer between higher-energy-gap materials, as in a standard double heterojunction, but with the low-energy-gap layer thickness set below the deBroglie wavelength of the electrons in the material. This results in quantum confinement of the electrons in the direction perpendicular to the growth plane, and in an elevation in energy of the lowest available electron energy states above the conduction band edge. The thinner the layer, the more the ground-state energy is elevated. The spatial overlap of the electron wavefunction into the high-energy barriers also increases with thinner layers. If the barrier material is chosen to have a lower mobility than the well material, then the mobility for electrons in the thinner wells will be less. The necessary configuration of low-energy high-mobility and high-energy low-mobility states can be designed by placing quantum wells of differing thicknesses in close proximity to one another. At

Manuscript received January 19, 1994; revised September 13, 1994. This work was supported by the Office of Naval Research.

The author is with the Naval Research Laboratory, Washington, D.C. 20375-5347 USA.

IEEE Log Number 9410337.

low applied electric fields, electrons populate the ground state energy levels of the widest quantum wells. As the applied field is increased, electrons gain sufficient energy to scatter into the higher states, thus populating the narrower wells of higher energy and lower mobility. The negative differential conductivity and nonlinear resistance associated with this effect should exist to very high frequencies, since the transit distances are very small and relaxation times involved are very short.

B. Microwave Conduction Considerations

The principle objective of this work has been to measure the microwave conduction properties of a specialized class of semiconductor heterostructures. It is necessary to be able to place the sample in interaction with a propagating microwave signal while simultaneously applying a constant electric dc-bias field to the sample. The special device geometry used to accomplish this is shown in Fig. 1(a). The device footprint covers a substrate area of 700 × 700 μm. This contains a 200 × 700-μm central active region upon which the coplanar stripline is fabricated. Two 300 × 300-μm ohmic contact regions are positioned on opposite sides of this central region to permit the application of the dc bias. A cross section of the device is shown in Fig. 1(b). The coplanar stripline is electrically isolated from the multiple-quantum well region by a 3000-Å-thick oxide layer. The coplanar striplines are made from an e-beam evaporator-deposited 1.5-μm-thick Ag layer, patterned in the lateral dimensions necessary to result in a 50-ohm transmission-line characteristic impedance. The coplanar stripline within the active region of the device consists of two 15-μm-wide strips separated by a 35-μm-wide gap. Outside of the active region, the coplanar stripline flares to 30-μm-wide strips with a 70-μm-wide separation. The flaring is necessary to provide for contact pads that are compatible with the employed microwave probe. This design results in two distinct interacting devices—the dc device consisting of the ohmic contacts and of the heterolayers necessary for ohmic contact formation and dc conduction, and the microwave device consisting of the coplanar-strip transmission line and the insulating and semiconducting layers that comprise its substrate. The only coupling between these two devices is through the interaction between fields associated with the propagating microwave signal along the transmission line and the heated electrons in the quantum wells. The steps required to fabricate this geometry are described below.

II. Device Design and Fabrication

A. Heterostructure Design

The heterostructure types that are of interest for these measurements are those which have been demonstrated to exhibit nonlinear conduction and negative differential conductivity at dc and low frequencies. A typical heterostructure of this kind utilizes a multi-level superlattice—a superlattice that is composed of repeated sequences of dissimilar quantum wells [5], [6]. Such a structure is usually realized using molecular beam epitaxy. One particular structure, which will be described in detail here, is shown in Fig. 2 and was grown by the

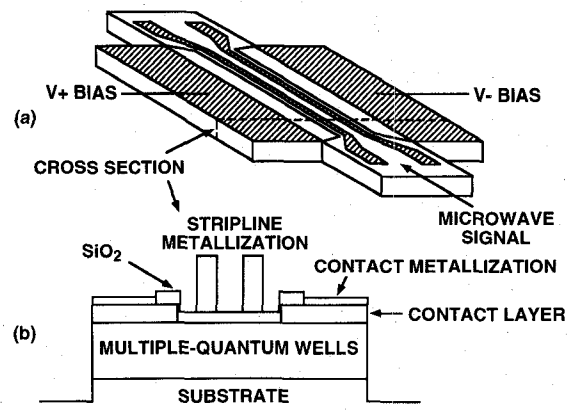

Fig. 1. (a) Coplanar stripline device, with (b) cross-section at dotted line, showing geometry of the device components.

following sequence as illustrated in Fig. 2(a): A 5000-Å-thick undoped GaAs layer is deposited initially on a semi-insulating GaAs substrate, followed by 2-μm-thick (10-period) superlattice with a unit cell composed of a 450-Å-thick GaAs region, a sequence of 140 Å, 70 Å, 50 Å, 70 Å, and 140 Å GaAs wells separated from one another by 80 Å $Al_{0.3}Ga_{0.7}As$ barriers, followed by a second 450-Å-thick GaAs layer. The conduction-band edge as a function of thickness as well as the relative positions of the ground state energies is shown in Fig. 2(b). The entire 2-μm-thick multi-quantum-well region is doped n-type with 10^{16} cm^{-3} Si. This level of doping has been determined to be the minimum necessary for ohmic conduction in the quantum well region. Ohmic conduction is important, since the applied bias must result in a uniform applied electric field in the quantum wells. Depletion effects and charge accumulations will result if the electric field is nonuniform, and will dominate the device conduction. Lower doping levels decrease the threshold for applied-bias-induced depletion pinch-off of the channel, and increase the effect of space-charge-limited-injection accumulations at the contacts. Higher doping levels result in addition power dissipation, which heats the device and degrades the high-field conduction nonlinearities. Degenerately-high doping levels can also result in such large carrier populations that the quantum well band-structure becomes swamped with electrons, and higher energy empty states necessary for real-space transfer are occupied. Thus, a doping level of about 10^{16} cm^{-3} Si is optimal for the superlattice. On top of this superlattice a 2500-Å-thick GaAs layer doped n-type with 10^{18} cm^{-3} Si is grown to permit easy formation of ohmic contacts. This device structure was originally chosen for the purposes of investigating the properties of the negative differential conductivity effect first observed in quantum-well electron barrier diodes [7], when similar multiple-quantum-well sequences are incorporated into a channel conduction device design. At low bias, electrons are present principally in the 450-Å-thick GaAs layers. As the electrons heat under high bias conditions, they scatter into the higher energy states of the adjacent quantum wells, where the combination of two-dimensional confinement and wavefunction overlap with the $Al_{0.3}Ga_{0.7}As$ barriers results in reduced mobility. This real-space shift in the population of electrons from high-mobility to low-mobility layers results

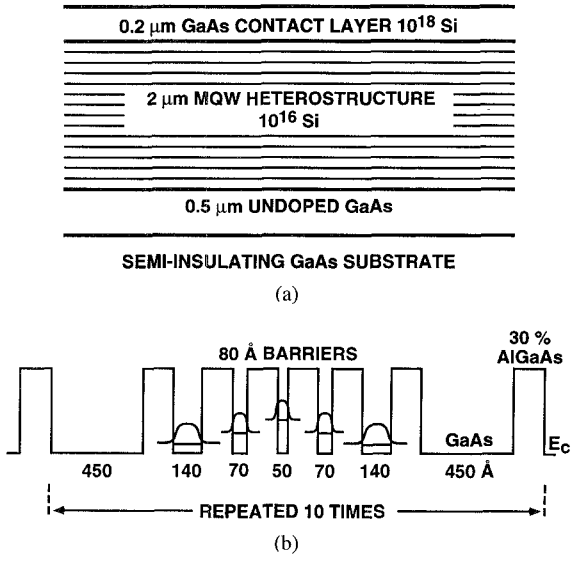

Fig. 2. (a) Heterostructure layers and (b) multiple-quantum-well geometry.

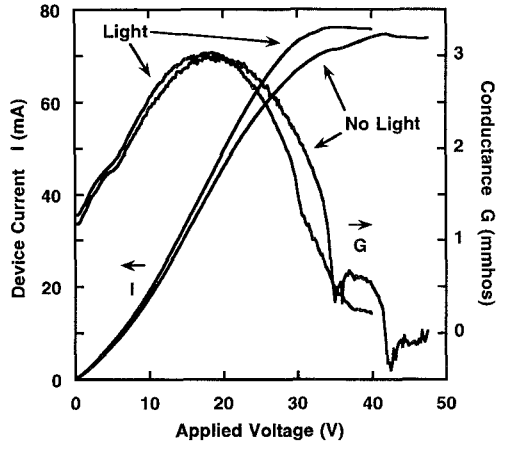

Fig. 3. Current (I) and conductance (G—measured at 1 KHz) as a function of voltage, taken from the dc contacts of the device.

in the observed negative differential conductivity as measured from the dc device terminals.

B. Device Fabrication

The devices were fabricated from the superlattice material using standard photolithographic techniques. Initially, the highly-doped contact layer had to be removed from between the ohmic contact regions to prevent the device from shorting out through this layer. This was accomplished by opening windows in Microposit 1350J photoresist, and then etching the contact layer off with a H_2O_2-NH_3OH selective etch. A layer of insulating SiO_2 was then sputter-deposited over the sample, and a second photoresist step was undertaken to remove the oxide layer from the ohmic contact regions and to pattern the Ni-Ge-Au ohmic contacts using photoresist liftoff. Another photoresist patterning step was performed to fabricate 1.5-μm-thick Ag coplanar stripline on the device. The strip metallization was deposited to a minimum thickness of 1.5 μm. A thickness on the order of a skin depth is necessary to keep microwave losses within acceptable bounds. A final photoresist step was used to cover the entire device structure and isolate it from the rest of the sample with a 2-μm-high mesa, etched with 5:1:1 H_2SO_4:H_2O_2:H_2O. The completed devices were subsequently mounted on copper heat sinks for testing.

III. Characterization and Measurement

A. Low-Frequency Measurements

Dc characterization of the completed devices was performed initially to determine the bias regimes of nonlinear conductivity and to test for basic device operation. The measurements were made using a lock-in amplifier conductance measuring technique [6], [8]. Dc probes were dropped on the ohmic contacts to permit electrical connection to the device. The device under test was connected in series with a 100-ohm current-sensing resistor. A 2-mV ac signal was superimposed on the applied dc, and the ac and dc voltages were measured across the device and the current-sensing resistor. Measurements were made from the dc-bias contacts and do not involve the coplanar stripline. Thus, direct one-for-one comparisons with the component values and equivalent circuit models determined from the high frequency measurements are not possible. The dc conductance measurements taken at 1 KHz and the current and conductance versus voltage characteristics for this heterostructure are shown in Fig. 3. This device experienced negative differential conductivity above 35 V of dc bias, and was observed to be slightly photoconductive due to the relatively low carrier concentrations present in the wells. It is also apparent that the negative differential conductivity observed under dc excitation does not manifest itself as negative conductivity as measured from the dc contact terminals at 1 KHz. This difference demonstrates that some portion of the dc nonlinearities have very low frequency limits, and emphasizes the importance of obtaining microwave data to determine the frequency response of these conductivity effects.

Additional measurements have been made of the low-frequency response using the same lock-in amplifier setup. Data was taken at discrete bias points, while sweeping the 2-mV ac frequency from 100 Hz–50 KHz. The equivalent circuit model which best matches to the low-frequency data is shown in Fig. 4, along with a plot of the variation of equivalent-circuit element values with bias. This equivalent circuit represents the channel region between the dc contacts, and the voltage dependence of the components represents a linear fit to the changing conduction properties of the channel as electrons scatter into higher energy states with increasing voltage. The inclusion of capacitance in this circuit is consistent with the energy storage effects observed in earlier devices [8]. These values are consistent with the dc current versus voltage characteristics of Fig. 3, although direct measurement of negative differential conductivity is not confirmed.

B. Microwave Measurements

Microwave characterization of these devices was conducted using a Cascade Microtech microwave probe station connected to an HP 8510 network analyzer. All microwave measurements

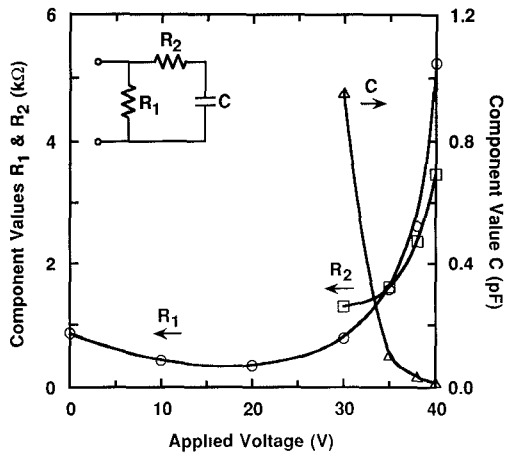

Fig. 4. Equivalent-circuit component values derived from low-frequency measurement (100 Hz–50 KHz) for the circuit shown in the inset.

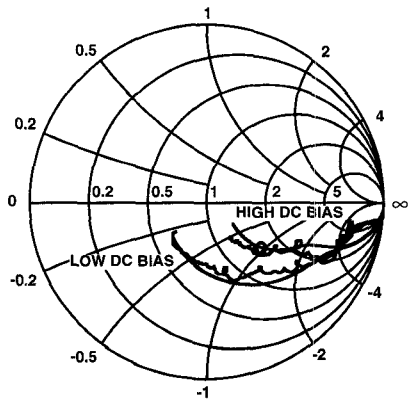

Fig. 5. Reflection data with calculated equivalent-circuit response for low (0 V) and high (41 V) dc device biases, beginning near the open circuit point for 50 MHz, and shifting toward the center of the chart as the frequency is increased to 10 GHz.

were made using the coplanar strip contacts, designed with the proper geometry to accommodate ground-signal probes. Dc bias was provided with the same equipment used to carry out the low-frequency measurements, and low-frequency conductivity was measured concurrently with the microwave conductivity in order to monitor the bias state of the device throughout the measurement cycle.

1) Open-circuit reflection measurements: Because of the insulating SiO_2 layer underlying the stripline, it is expected that a simple lumped element model of this device would be dominated by a series capacitor. This leads to the conclusion that any conductivity changes in the multiple quantum wells will be most strongly observed in an open circuit reflection measurement. Such measurements have been conducted in the frequency range from 45 MHz–20 GHz. Fig. 5 shows the reflection coefficient data (S11) for a frequency range from 45 MHz–10 GHz with low- and high-bias states plotted on a Smith Chart. This verifies the large effect of device bias on the observed impedance of the coplanar stripline. Calculated curves are also shown in Fig. 5 for the equivalent circuit shown in the inset of Fig. 6. This model fit is represented by the smooth lines that overly the much less smooth data lines of Fig. 5. At low frequencies, nearly all of the signal is reflected, resulting in data points near the open circuit point on the Smith Chart. This is expected, since the oxide layer is capacitive in its effect and presents a high series impedance which reduces the interaction with the quantum-well layers at low frequencies. As the excitation frequency is increased, the data points move toward the center of the chart. At no frequency or dc bias does the data move outside the unit circle, as might be expected in the presence of negative differential conductivity. Fig. 6 summarizes the equivalent circuit element values for the complete data set as a function of applied bias. The fixed 3-pF capacitance is due to the insulating oxide layer underlying the coplanar stripline. The 150-ohm fixed resistor is a leakage path to ground. The variable resistor and capacitor represent the quantum well region. The voltage dependence of the variable resistance is consistent with the dc and low frequency ac results. Direct observation of negative differential conductivity appears to occur only in the dc regime

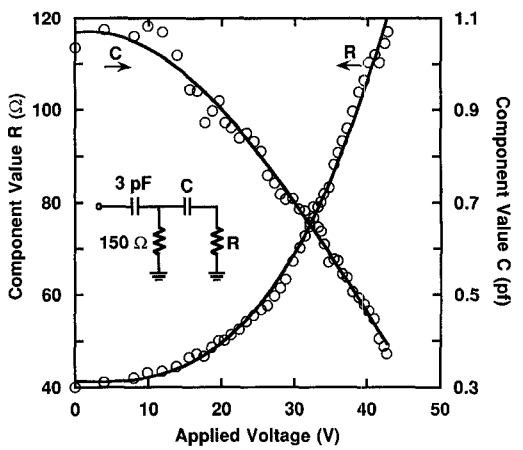

Fig. 6. Equivalent-circuit component values derived from reflection measurements for the circuit shown in the inset.

for this particular device. The variable capacitance seen here is consistent with low-frequency data observations, and is expected to originate from interactions between the heated electron populations in the adjacent quantum wells [8].

2) Transmission measurements: Interaction between the substrate under bias and the overlying microwave coplanar stripline has been observed in transmission measurements, as well. Fig. 7(a) shows the transmission coefficient plotted for the low-bias state and Fig. 7(b) shows the transmission data for the high-bias state of this device. The smooth lines of Fig. 7 represent calculated model fittings, based on a standard model developed by EESof for use in transmission line design, to the less-smooth experimental data. At low frequencies, the transmission is near unity, resulting in data points near the unity-transmission point on the transmission coefficient plane. As the frequency is increased, coupling to the substrate through the insulating oxide layer results in microwave loss, causing the measured data to move toward the center of the chart. The changes in transmission with applied dc bias are relatively small. This is to be expected given the small degree of field overlap with the superlattice layers. Yet, this data clearly demonstrates bias-dependent interaction between the multiple quantum wells and the microwave coplanar line. As

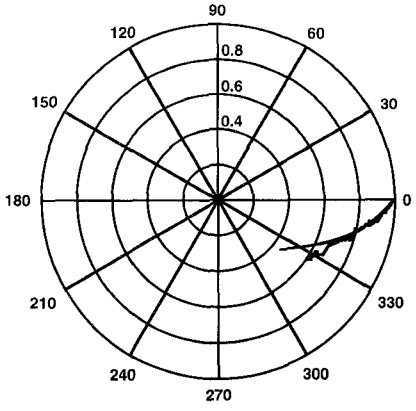

(a)

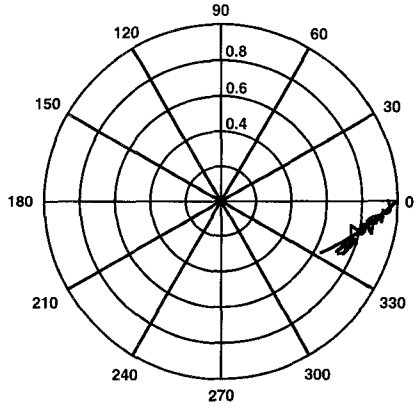

(b)

Fig. 7. Transmission data with calculated equivalent-circuit response for (a) low (0 V) and (b) high (46 V) dc device biases, beginning near the unity transmission point for 50 MHz, and shifting toward the center of the chart as the frequency is increased to 12 GHz.

bias is applied, the data shifts away from the center of the chart. This means that the microwave losses present at low dc bias are reduced at high dc bias, as would be expected as the superlattice conductivity decreases with applied dc bias. A standard numerical design model for coplanar lines has been utilized to model this data. Appropriate physical dimensions and substrate parameters corresponding to the actual device design were used. In order to account for the coplanar line flaring necessary for matching to the probe spacing, a series capacitor-resistor pair is added to both ports of the coplanar stripline model. The bias dependence of the tuning capacitor as well as the substrate loss tangent determined by fitting to the measured data are shown in Fig. 8. A change in loss tangent from 8 to 5 is observed over the dc-bias range of the measurement. These numbers are only crudely applicable to the actual geometry of this experiment, since the model employed assumes a homogeneous substrate composition, which is obviously not the case here. However, the trend in the data is clearly observed, and the resulting reduction in loss tangent is consistent with the measured conductivity changes in the device at dc and low frequencies. These data are also consistent with the reflection coefficient data measured over the same frequency range in the open-circuit measurements of Figs. 6 and 7.

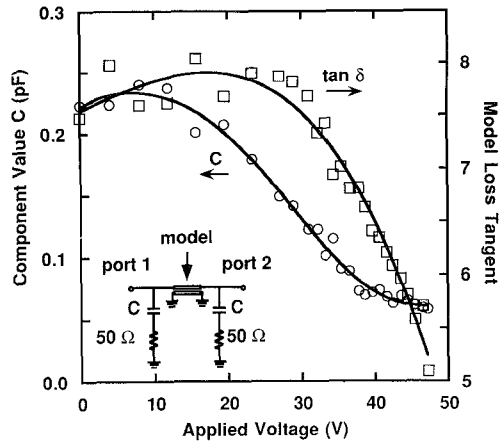

Fig. 8. Equivalent-circuit component values calculated from transmission measurements for the circuit shown in the inset.

IV. Conclusion

A novel coplanar stripline device design as been used to investigate microwave interactions in a multiple-quantum-well GaAs-AlGaAs heterostructure under applied dc bias. Correlation between the dc terminal characteristics of this structure under bias and changes in the microwave properties of the overlying coupled transmission line have been demonstrated. The microwave data correlates well with the low-frequency characteristics of the device, showing that the nonlinear conduction effects present at low frequencies extend into the microwave range to at least 20 GHz. This new device concept is attractive due to the high degree of flexibility in both the heterostructure and microwave considerations of the design. Variations of this device can be optimized for use as microwave mixers, detectors, or other applications which can exploit these nonlinear conduction effects.

Acknowledgment

The author would like to acknowledge the technical support of D. S. Katzer and the helpful technical discussions of H. S. Newman, J. M. Pond, and C. Rauscher.

References

[1] J. M. Pond, S. W. Kirchoefer, and E. J. Cukauskas, "Microwave amplification to 2.5 GHz in a quantum state transfer device," *Appl. Phys. Lett.*, vol. 47, pp. 1175–1177, Dec. 1985.

[2] A. Straw, A. Da Cunha, N. Balkan, and B. K. Ridley, "Negative Differential Resistance, High Field Domains, and Microwave Emission in GaAs Multi-Quantum Wells," in *Negative Differential Resistance and Instabilities in 2-D Semiconductors*. NATO ASI Series B, Physics, vol. 30, N. Balkan, B. K. Ridley, and A. J. Vickers, Eds. New York: Plenum, 1993.

[3] K. Hess, H. Morkoc, H. Shichijo, and B. G. Streetman, "Negative differential resistance through real-space electron transfer," *Appl. Phys. Lett.*, vol. 35, pp. 469–471, Sept. 1979.

[4] P. D. Coleman, J. Freeman, H. Morkoc, K. Hess, B. G. Streetman, and M. Keever, "Demonstration of a new oscillator based on real-space transfer in heterojunctions," *Appl. Phys. Lett.*, vol. 40, pp. 493–495, Mar. 1982.

[5] S. W. Kirchoefer, R. Magno, and J. Comas, "Negative differential resistance at 300K in a superlattice quantum state transfer device," *Appl. Phys. Lett.*, vol. 44, pp. 1054–1056, June 1984.

[6] S. W. Kirchoefer, "Negative differential resistance in superlattice and heterojunction channel conduction devices," in *Negative Differential Resistance and Instabilities in 2-D Semiconductors,* NATO ASI Series B, Physics, vol. 307, N. Balkan, B. K. Ridley, and A. J. Vickers, Eds. New York: Plenum, 1993.
[7] H. S. Newman and S. W. Kirchoefer, "Electronic properties of symmetric and asymmetric quantum-well electron barrier diodes," *J. Appl. Phys.,* vol. 62, pp. 706–710, July 1987.
[8] S. W. Kirchoefer, "Occupation of quantum states determined by energy storage in superlattice quantum state transfer devices," *Appl. Phys. Lett.,* vol. 57, pp. 1143–1145, Sept. 1990.

Steven W. Kirchoefer (S'81–M'82) was born in St. Louis, MO, on Oct. 18, 1955. He received the B.S., M.S., and Ph.D. degrees, all in electrical engineering, from the University of Illinois in 1978, 1979, and 1982, respectively.

From 1982 to the present, he has been employed by the U.S. Naval Research Laboratory in Washington, D.C. His work there has involved the use of compound semiconductor technology for high speed device applications. He has fabricated and demonstrated many prototype device designs utilizing the properties of carriers confined to thin heterolayers. Among these are various types of electron barrier devices, real space transfer effect devices, various specialized devices for the study of tunneling effects, doping interactions, and optical interactions in quantum–well structures, and device structures for the study of microwave interactions in multiple quantum–well heterostructures and superlattices.

Dr. Kirchoefer is a member of the American Physical Society.